RESEARCH ARTICLE | NOVEMBER 17 2023

Characterization of D-T generator neutron flux spectrum for cyclic neutron activation analysis experiments

S. M. Lyons ; B. D. Pierson; M. Mayfield; J. Christ; C. A. Lani; M. Flaska

AIP Conf. Proc. 3040, 070003 (2023)
https://doi.org/10.1063/5.0176948

Characterization of D-T Generator Neutron Flux Spectrum for Cyclic Neutron Activation Analysis Experiments

S. M. Lyons,[1, a)] B. D. Pierson,[1] M. Mayfield,[1] J. Christ,[1] C. A. Lani,[2] and M. Flaska[2]

[1]*Pacific Northwest National Laboratory, 902 Battelle Blvd., Richland, Washington 99354*
[2]*Ken and Mary Alice Lindquist Department of Nuclear Engineering, Pennsylvania State University, State College, Pennsylvania*

[a)]Corresponding author: stephanie.lyons@pnnl.gov

Abstract. Improving nuclear data for short-lived fission product yields will further our fundamental understanding of fission, which is needed across various scientific fields and applications. One method of attaining the needed product yield data is through cyclic neutron activation, which allows a target to be irradiated in a neutron environment and then transported for counting of the radionuclides produced, typically via γ spectroscopy. Recently, such a system was constructed and commissioned at Pacific Northwest National Laboratory. In this system, targets are shuttled between the head of a D-T neutron generator and a counting station with a transit time of about 2 sec. As part of the characterization of this system, the neutron flux was studied using two activation targets. The neutron flux from the deuterium-tritium fusion generator was determined to be $9.95 \pm 0.33 \times 10^8$ n/cm^2·s with a peak energy of 14.9 MeV and a spread of approximately 4 decades between the epithermal and 14 MeV peak group flux.

INTRODUCTION

Fission product yield data available from common nuclear data sources such as the Evaluated Nuclear Data File have not been updated since the last evaluation by England and Rider in 1994 [1]. Modern fission product yield data were identified as representing a nuclear data gap during the Nuclear Data Roadmapping and Enhancement Workshop (NDREW) in 2018 [2], which has spurred an international review of the available fission product yield data and fission models for the release of a new evaluation expected by 2025. This effort aims to modernize the evaluation by replacing the historic England and Rider fission model with a more complete model of the fission process [3, 4]. More fission product yields are needed to constrain and refine parameter convergence of modern fission product yield models. The new evaluation will mostly, if not entirely, consist of model-predicted yields with the exception of peak product yields, such as ^{99}Mo, ^{104}Ru, and ^{95,97}Zr. For further improvement, more experimental data, specifically short-lived fission product yields, are needed. The data not only further the fundamental understanding of the fission process that underpins these models, but the measured yields are needed for nuclear astrophysics, reactor physics, and materials safeguards.

Cyclic neutron activation analysis (CNAA) has long been used to measure various cross sections as well as neutron-induced fission yields on various actinides [5, 6]. CNAA is a technique that leverages the high specific activity of short-lived radionuclides by repeatedly activating and counting a sample [7, 8]. Coupling CNAA with a pneumatic rabbit system allows for rapid transport of the target between a neutron source, such as a D-T fusion neutron generator, and a counting station, enabling short-lived products ($T_{1/2} \approx 1$ sec) to be studied [6]. The critical requirements of the CNAA method are consistency in the timing, repetition, and radiation exposure field used during the experiment. This report describes measurements conducted to evaluate the consistency of the as-built system.

METHODS

A cyclic neutron activation analysis pneumatic system (CNAAPS) was constructed at Pacific Northwest National Laboratory (PNNL) to study short-lived fission product yields. CNAAPS uses a pneumatic transfer tube to transport samples from the head of a Thermo Scientific D711 D-T neutron generator to a shielded counting station consisting of two 110% relative efficiency p-type high-purity Ge detectors. CNAAPS is controlled by an Arduino/Intel Windows 7 unit for a single unified acquisition clock. Data acquisition from the detectors is performed by a CAEN Hexagon dual channel digital multi-channel analyzer. Surge tanks are used at both ends of the system to improve the consistency of sample transit. The timing performance of CNAAPS was tested as part of the commissioning of the system. The shortest sample transfer time achievable was 1.836±0.054 sec. However, this was accomplished using the maximum operating speed and resulted in increased target deformation. An air buffer was developed to prolong the capsule

AIP Conf. Proc. 3040, 070003-1–070003-4; https://doi.org/10.1063/5.0176948
Published by AIP Publishing. 978-0-7354-4718-9/$30.00

life-time, resulting in sample transit time from the generator to the detectors in 2.150 $\pm$ 0.062 sec as shown in Figure 1.

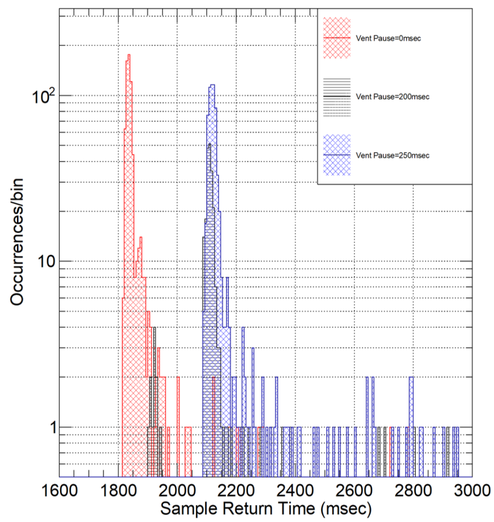

FIGURE 1. Resultant transit time of CNAAPS capsule with varying air buffer delay times: 0 msec, 200 msec, and 250 msec.

Two types of targets were fabricated to characterize the neutron flux spectrum for CNAAPS: one focusing on short-lived isotopes to investigate the repeatability and provide a rough estimate of the neutron-energy profile (short-lived target), and one focused on long-lived isotopes with a mixture of 14 metal compounds leveraging over 20 possible reactions for characterization (long-lived target).

Table 1 details the composition of the two targets and the reactions used in the analysis. The masses of the various chemical compounds listed in Table 1 were compressed and heat sealed in an internal polyethylene target. The internal capsule was contained in a high-density polyethylene overpack, which was heat-sealed as well, and rated for 500 cycles.

The short-lived target was used for three cycles of 30-min irradiations at the face of the neutron generator and 150-min counts. The longer count time between irradiations allowed the short-lived products to decay before the next cycle, yielding a good test in irradiation repeatability. Using ^{19}O ($T_{1/2}$ = 26.9 sec [9]), the observed variation in activity was 3.6% for the three cycles. This is important for the future short-lived fission product experiments, which will require hundreds of irradiation and counting cycles to build the necessary statistics for accurate analysis. The long-lived target was irradiated for 7 hr at the face of the neutron generator. The target was then counted immediately after and again at several time intervals. As can be seen in Table 1, the half-life for several of the observed products was several days long, enabling the target measurement to be repeated several times. The data from both the short- and long-lived targets were used to perform two independent characterizations of the neutron flux for CNAAPS.

RESULTS AND CONCLUSIONS

The resultant spectra from the short- and long-lived target experiments were analyzed and the activity per gram determined for the reactions of interest, listed in Table 1. The activities were then analyzed in the STAYSL PNNL SigPhi Calculator, which calculates the neutron activation rate from the measured activity correcting for photon and neutron self-attenuation [10]. These reaction rates, or $\sigma \cdot \phi$, represent the spectral averaged cross-sections folded with the total neutron fluence. The rates determined from the analysis of the short- and long-lived targets are given in Table 1 and contain $\leq$7% error based on the uncertainty in the activity. The rates are used as input for the STAYSL PNNL spectral adjustment, which uses a least-squares fitting method to adjust and optimize an MCNP estimate of the neutron flux spectrum [10].

The results from the STAYSL PNNL evaluation of the two characterization targets are shown in Figure 2 and tabulated in Table 2. A total of six reactions were used in the evaluation of the short-lived target, and 16 reactions

TABLE 1. Composition details for the short- and long-lived targets and the reactions used for the characterization of the D-T neutron generator neutron flux spectrum for CNAAPS, including determined rates ($\sigma \cdot \phi$).

Target	Compound	Mass (mg)	Reaction	$T_{1/2}$	E_γ (keV)	$\sigma \cdot \phi(\frac{atoms_{prod}}{atoms_{targ}/s})$
Short-lived	Al_2O_3	19.87	^{27}Al(n,α)^{24}Na	14.95 hr	1,368.0	1.17×10^{-16}
			^{27}Al(n,p)^{27}Mg	9.46 min	843.0	2.12×10^{-17}
	Fe_2O_3	22.18	^{56}Fe(n,p)^{56}Mn	154.73 min	847.0	3.48×10^{-17}
	HgS	83.89	^{199}Hg(n,n')^{199m}Hg	42.67 min	158.3	2.17×10^{-16}
	$In(OH)_3$	20.07	^{115}In(n,g)^{116m}In	54.26 min	1,293.6	7.44×10^{-17}
			^{115}In(n,n')^{115m}In	4.49 hr	336.2	5.87×10^{-17}
			^{115}In(n,2n)^{114m}In	49.51 days	190.3	3.49×10^{-15}
	PbF_2	173.88	^{204}Pb(n,n')^{204m}Pb	68.40 min	899.0	2.01×10^{-17}
			^{19}F(n,2n)^{18}F	109.75 min	511.0	1.55×10^{-17}
	SiO_2	2.97	^{28}Si(n,p)^{28}Al	134.48 sec	1,778.9	8.06×10^{-17}
Long-lived	AgI	27.86	^{127}I(n,2n)^{126}I	12.93 days	666.0	5.54×10^{-16}
	Au	3	^{197}Au(n,γ)^{198}Au	64.70 hr	411.8	1.03×10^{-16}
			^{197}Au(n,2n)^{196}Au	6.17 days	355.7	7.88×10^{-16}
	Fe_2O_3	19.69	^{54}Fe(n,p)^{54}Mn	312.20 days	834.8	1.31×10^{-16}
			^{54}Fe(n,α)^{51}Cr	27.70 days	320.0	3.73×10^{-17}
			^{56}Fe(n,p)^{56}Mn	154.73 min	846.7	3.58×10^{-17}
	HgS	10.47				
	$In(OH)_3$	7.08	^{113}In(n,n')^{113m}In	99.48 min	391.7	4.20×10^{-17}
			^{115}In(n,2n)^{114m}In	49.51 days	558.0	5.07×10^{-16}
			^{115}In(n,n')^{115m}In	4.49 hr	336.2	4.88×10^{-17}
			^{115}In(n,γ)^{116m}In	54.29 min	1,293.6	9.87×10^{-17}
	La_2O_3	20.47	^{139}La(n,γ)^{140}La	40.27 hr	815.8	3.23×10^{-18}
	Nb_2O_5	6.48				
	PbF_2	20.03	^{204}Pb(n,n')^{204m}Pb	68.40 min	374.7	5.78×10^{-21}
	SiO_2	2.84	^{28}Si(n,p)^{28}Al	134.48 sec	1,778.9	8.82×10^{-17}
	Ta_2O_5	33.19				
	TiO_2	19.17	^{46}Ti(n,p)^{46}Sc	83.79 days	889.3	1.09×10^{-16}
			^{48}Ti(n,p)^{48}Sc	43.67 hr	1,037.5	2.81×10^{-17}
	WO_3	23.76	^{186}W(n,γ)^{187}W	23.72 hr	685.8	3.79×10^{-17}
	ZnO	11.13	^{67}Zn(n,p)^{67}Cu	61.83 hr	184.6	2.38×10^{-17}
	ZrO_2	12.2	^{90}Zr(n,2n)^{89}Zr	78.41 hr	909.1	2.70×10^{-16}

TABLE 2. Resultant group-flux from STAYSL PNNL CNAAPS evaluation.

Energy (MeV)	Flux from Short-Lived Target (n/cm^2·s)	Flux from Long-Lived Target (n/cm^2·s)
$1.00 \times 10^{-10} - 5.50 \times 10^{-7}$	$0.58 \pm 3.34 \times 10^5$	$8.93 \pm 4.68 \times 10^4$
$5.50 \times 10^{-7} - 1.00 \times 10^{-4}$	$2.27 \pm 8.12 \times 10^5$	$3.47 \pm 0.41 \times 10^5$
$1.00 \times 10^{-4} - 1.10 \times 10^{-1}$	$4.50 \pm 1.70 \times 10^6$	$6.15 \pm 1.49 \times 10^6$
$1.10 \times 10^{-1} - 1.00 \times 10^0$	$1.82 \pm 0.39 \times 10^6$	$2.40 \pm 0.37 \times 10^6$
$1.00 \times 10^0 - 1.00 \times 10^1$	$4.02 \pm 0.68 \times 10^7$	$7.71 \pm 0.54 \times 10^7$
$1.00 \times 10^1 - 1.20 \times 10^1$	$3.74 \pm 0.73 \times 10^6$	$6.77 \pm 0.70 \times 10^6$
$1.20 \times 10^1 - 1.30 \times 10^1$	$3.86 \pm 0.70 \times 10^6$	$5.94 \pm 0.56 \times 10^6$
$1.30 \times 10^1 - 1.40 \times 10^1$	$5.62 \pm 0.91 \times 10^6$	$7.11 \pm 0.58 \times 10^6$
$1.40 \times 10^1 - 1.65 \times 10^1$	$3.03 \pm 0.06 \times 10^8$	$3.54 \pm 0.04 \times 10^8$

were used in the evaluation of the long-lived target. The plots show the expected neutron lethargy, which is defined as flux (ϕ) times the energy (δE), from the D-T fusion generator, the adjusted neutron lethargy from the analysis, and the percent difference. The results of the short-lived target demonstrate excellent agreement with simulations, varying

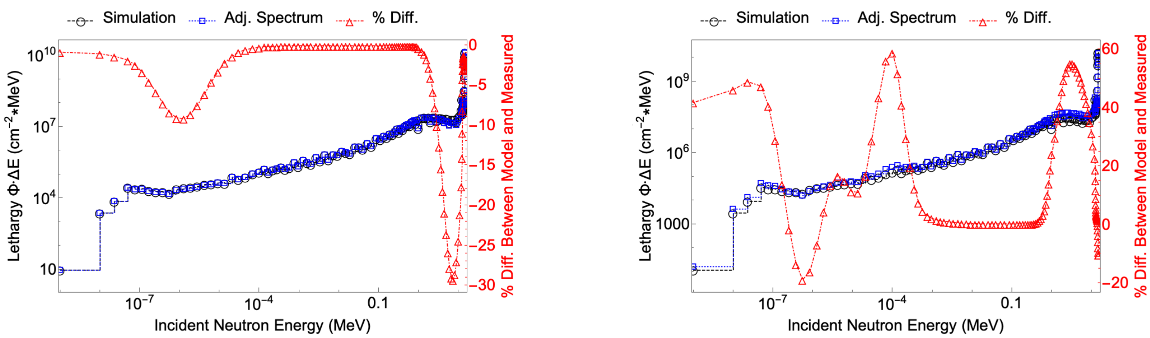

Short-lived target results

Long-lived target results

FIGURE 2. Results from the STAYSL PNNL evaluations for the two characterization targets. The black points are from simulations of the expected flux in lethargy (cm^{-2} × MeV), the blue squares are the resultant adjusted flux from STAYSL PNNL, and the red triangles show the percent difference.

by a maximum of 30% right below the 14 MeV peak. The long-lived target results show more variation in the results, with a maximum difference of 60% in the epithermal region and near 60% below the 14 MeV peak. The completed neutron flux characterization for CNAAPS provides necessary data for the determination of fission product yields and cross sections.

ACKNOWLEDGMENTS

This material is based upon work supported by the US Department of Defense, Defense Threat Reduction Agency, Grant No. 12393672.

REFERENCES

1. T. England and B. Rider, "Evaluation and compilation of fission yields," ENDF-349, LA-UR-94-3106 (1994).
2. C. E. Romano, T. Ault, L. Bernstein, R. Bahran, B. T. Rearden, P. Talou, *et al.*, "Proceedings of the Nuclear Data Roadmapping and Enhancement Workshop (NDREW) for Nonproliferation," (2018), 10.2172/1465032.
3. K. H. Schmidt, B. Jurado, C. Amouroux, and C. Schmitt, "General description of fission observables: GEF model code," Nucl. Data Sheets **131**, 107–221 (2016).
4. T. Kawano and M. B. Chadwick, "Estimation of ^{239}Pu independent and cumulative fission product yields from the chain yield data using a Bayesian technique," J. Nucl. Sci. Technol. **50**, 1034–1042 (2013).
5. M. Al-Mugrabi and N. Spyrou, "The determination of uranium using short-lived fission products by cyclic and other modes of activation analysis," J. Radioanal. Nucl. Chem. **112**, 277 – 283 (1987).
6. B. D. Pierson, L. R. Greenwood, M. Flaska, and S. A. Pozzi, "Fission product yields from ^{232}Th, ^{238}U, and ^{235}U using 14 MeV neutrons," Nucl. Data Sheets **139**, 171–189 (2017), special Issue on Nuclear Reaction Data.
7. H. Dung, M. Blaauw, D. Beasley, and M. D. C. Freitas, "Development of the k_0-based cyclic neutron activation analysis for short-lived radionuclides," J. Radioanal. Nucl. Chem. **291**, 485–492 (2012).
8. R. R. Greenberg, P. Bode, and E. A. De Nadai Fernandes, "Neutron activation analysis: A primary method of measurement," Spectrochim. Acta B **66**, 193–241 (2011).
9. D. R. Tilley, H. R. Weller, C. M. Cheves, and R. M. Chasteler, "Energy levels of light nuclei a = 18–19," Nucl. Phys. A **595**, 1–170 (1995).
10. L. R. Greenwood and C. D. Johnson, "STAYSL PNNL Suite," [Computer Software] `https://doi.org/10.11578/dc.20210521.51` (2013).